Available online at www.sciencedirect.com
ScienceDirect
Journal of Computational Physics 227 (2008) 2970–2976
JOURNAL OF COMPUTATIONAL PHYSICS
www.elsevier.com/locate/jcp

Precise numerical solutions of potential problems using the Crank–Nicolson method

Daekyoung Kang, E. Won *

Department of Physics, Korea University, Seoul 136-713, Republic of Korea

Received 12 October 2006; received in revised form 3 April 2007; accepted 21 November 2007
Available online 4 December 2007

Abstract

We present a numerically precise treatment of the Crank–Nicolson method with an imaginary time evolution operator in order to solve the Schrödinger equation. The time evolution technique is applied to the inverse-iteration method that provides a systematic way to calculate not only eigenvalues of the ground-state but also of the excited-states. This method systematically produces eigenvalues with the accuracy of eleven digits when the Cornell potential is used. An absolute error estimation technique is implemented based on a power counting rule. This method is examined on exactly solvable problems and produces the numerical accuracy down to 10^{-11}.

Keywords: Crank–Nicolson method; Precise numerical calculation; Finite differences; Imaginary time; Schrödinger equation

---

1. Introduction

Numerical computation of analytically unsolvable Schrödinger equations has been of interest in atomic and molecular physics, quantum chromodynamics, Bose–Einstein condensation of trapped atomic vapors, and plasma physics [1–6]. Conventionally, a wave function has been represented as a linear combination of plane waves or of atomic orbitals [7]. However, these representations entail high computational cost to calculate the matrix elements for these bases. Also, the plane wave bases set is not suitable for localized orbitals and the atomic orbital bases set is not suitable for spreading waves. In particular, the potential problems such as the Cornell potential [8,9] are difficult to solve in order to obtain precise eigenvalues because they have singularities at 0 and at ∞. Also, the potential includes non-perturbative regime when the linear term is significant.

To overcome these problems, numerical methods such as the Landé subtraction [10] and the Nystrom plus correction [11] in the momentum space have produced eigenvalues with six or seven meaningful digits. Other methods have adopted real-space representation [12,13]. In this method, a wave function is discretized by grid points in real-space providing from five to seven digits. Also, estimates using the exact solutions of the

---

[*] Corresponding author. Tel.: +82 2 3290 3113; fax: +82 2 927 3292.
E-mail addresses: windblue01@korea.ac.kr (D. Kang), eunilwon@korea.ac.kr (E. Won).

0021-9991/$ - see front matter © 2007 Elsevier Inc. All rights reserved.
doi:10.1016/j.jcp.2007.11.028

Killingbeck potential, have produced eigenvalues with seven digits [3]. Among these real-space methods, a method called the Crank–Nicolson (C–N) scheme [14–16] is known to be especially useful for one-dimensional systems because this method conserves the norm of the wave function exactly. Also, the computation is known to be stable and accurate even with a long time slice. These characteristics are very attractive for solving the Cornell potential problem. On the other hand, the current numerical precisions in solutions of the Cornell potential problem may not be as high as we would hope to achieve. For example, this lack of precision may forbid us to study fine or hyper-fine structure effects in the atomic system [10]. The calculation of matrix elements subject to large subtractions may require high accuracy in quantum chromodynamics [17]. Also, none of the references we compiled for this study contains a serious error estimate for their numerical calculations, when such error estimate is an important indicator of the reliability of a suggested numerical method. These two issues motivated us to solve the Cornell potential problem more precisely with a rigorous error estimate.

In this paper, we discuss our application of the C–N method to solve the Schrödinger equation with the Cornell potential. The radial part of the Schrödinger equation with the Cornell potential is given by

$$\left[-\frac{\mathrm{d}^2}{\mathrm{d}\rho^2}+\frac{\ell(\ell+1)}{\rho^2}-\frac{\lambda}{\rho}+\rho\right]u(\rho)=\zeta u(\rho), \tag{1}$$

where the dimensionless wave function $u(\rho)$, the orbital angular momentum quantum number ℓ, and the dimensionless energy eigenvalue ζ in Eq. (1) are described in Ref. [8]. The parameter λ is the relative strength between the Coulomb and the linear potentials, and we call it the Coulombic parameter throughout this paper. We present two different numerical methods in solving Eq. (1). First, the C–N method with the imaginary time evolution operator is re-interpreted by extending its allowed region. This may have used in practice earlier, but we explicitly describe it here to clarify our technique. This method produces ground-state eigenvalues with numerical accuracies of eleven digits when the Cornell potential is used. We then apply the original C–N time evolution technique to the inverse-iteration method [18]. This technique provides a systematic way to calculate not only the eigenvalue of the ground-state but also those of excited-states with less computational time by a factor of 10, while providing the same accuracy as in our re-interpreted C–N method. At the end of this paper, we discuss a mathematically simple but rigorous absolute error estimation for the numerical calculations.

2. The relaxed Crank–Nicolson method

The C–N method [14–16] is a finite difference method used for solving diffusive initial-value problems numerically. The main part of this method is the time evolution operation and the evolution operator for the Schrödinger equation may be approximated by the Cayley's form [7] as

$$\mathrm{e}^{-\mathrm{i}\mathcal{H}t}=\frac{1-\frac{\mathrm{i}}{2}\mathcal{H}t}{1+\frac{\mathrm{i}}{2}\mathcal{H}t}+\mathcal{O}(\mathcal{H}^3t^3), \tag{2}$$

where $\mathcal{H}$ is the Hamiltonian of the problem to be solved. This equality is correct up to the second order in $\mathcal{H}t$ and the approximation is valid when $|\mathcal{H}t|\ll 1$. By applying this operator to an initial wave function, the time-evolved wave function can be obtained. The standard C–N method makes use of Eq. (2) in order to study the time evolution of the wave function [14,15].

As a next step, we introduce the imaginary time method [4] to calculate the eigenfunctions and eigenvalues. By the Wick rotation, t is replaced by $-\mathrm{i}\tau$ in the time evolution operator [4]. This transforms the original Schrödinger equation into a diffusion equation. Then the wave function evolves in time slice Δt as

$$u(\rho,\Delta t)=\sum_{i=1}^{\infty}C_iu_i(\rho)\mathrm{e}^{-\mathrm{i}\zeta_i\Delta t}=\sum_{i=1}^{\infty}C_iu_i(\rho)\mathrm{e}^{-\zeta_i\Delta\tau}, \tag{3}$$

where $u_i(\rho)$ and ζ_i are the eigenfunction and the eigenvalue for the ith state, respectively. C_i is the relative amplitude for the ith state. The summation is over all possible eigenstates of the system.

For the imaginary time version, the eigenfunctions decay monotonically in time until the steady-state is reached. Here, rescaling of the wave function is required during the time evolution in order to preserve the

Table 1
Dependence of the ground-state eigenvalues ζ on the Coulombic parameter λ

λ	ζ (Ref. [8])	ζ (this work)	$\Delta\zeta$
0.0	2.338 107	2.338 107 410 458 750	1.0×10^{-12}
0.2	2.167 316	2.167 316 208 771 731	1.0×10^{-12}
0.4	1.988 504	1.988 503 899 749 943	9.6×10^{-13}
0.6	1.801 074	1.801 073 805 646 145	8.5×10^{-13}
0.8	1.604 410	1.604 408 543 235 973	6.6×10^{-13}
1.0	1.397 877	1.397 875 641 659 578	3.8×10^{-13}
1.2	1.180 836	1.180 833 939 744 863	2.1×10^{-14}
1.4	0.952 644	0.952 640 495 219 193	5.8×10^{-13}
1.6	0.712 662	0.712 657 680 462 421	1.3×10^{-12}
1.8	0.460 266	0.460 260 113 875 977	2.3×10^{-12}

The Cornell potential is used in the calculation. The second column contains the numerical results from Ref. [8] and the third column contains our result with the relaxed C–N method. The number of grid points is set to be $N = 300{,}000$ and $\Delta\tau = -5$ for the numerical analysis. An estimate on the numerical errors of the computation $\Delta\zeta$ is also listed at the last column and will be discussed later.

norm to be unity. The ground-state eigenvalue can then be read off from the steady-state eigenfunction as $\tau \to \infty$ [4]. Therefore, the time evolution operation itself in the C–N method acts as a tool that selects the ground-state exclusively, and the condition $|\mathcal{H}\tau| \ll 1$ is not absolutely necessary in the calculation of the ground-state eigenvalue. When all the eigenvalues are negative such as in the pure Coulomb potential, where $\zeta_0 < \cdots < \zeta_n < \cdots < 0$, the amplification of the ground-state coefficient may happen in the region $-2 < \mathcal{H}\tau < 0$ as the time evolution continues. On the other hand, when all the eigenvalues are positive such as in problems with the linear and Cornell potentials, where $0 < \zeta_0 < \cdots < \zeta_n$, the time evolution operator can amplify the ground-state coefficient in the region $\mathcal{H}\tau < -2$. Again, the condition $|\mathcal{H}\tau| \ll 1$ is not absolutely necessary and such a condition may be relaxed in order to obtain faster convergence to the ground-state eigenfunction. This relaxation of the convergence condition has been used in practice and we call this approach the *relaxed C–N method* throughout the paper.

Once the ground-state wave function is obtained, we can obtain the ground-state eigenvalue from the expectation value of the Hamiltonian of interest. Note that, for the numerical computation of an expectation value, the upper bound of the integral can not be infinity but rather a cut-off value, $\rho_{\max}$. We will explain how to control the numerical error produced by ignoring the region $(\rho_{\max}, \infty)$ later.

We applied the relaxed C–N method to the Cornell potential problem. We chose a Gaussian function as an initial wave packet. We did this because it contained contributions from the eigenstates that were being sought [8,9]. The λ dependence of the ground-state eigenvalues in Ref. [8] was reproduced with our relaxed C–N method and a comparison of the two results is summarized in Table 1. We also did a rigorous error analysis for our study and the results are included in the table. The error analysis will be explained in the later section. The time evolution in our relaxed C–N method gives eigenvalues over iterations down to stable 16-digits. All agree reasonably well with the results in Ref. [8]. For higher values of λ, the agreements become worse but we argue that our numbers are more precise as the error estimation of the numerical calculations are given in our computation. We also found that the convergence speed was improved by 10 times when it was compared with the standard C–N method that we tested. For excited-states, we can, in principle, obtain the eigenvalues from the lowest to higher-states by the Gram–Schmidt orthogonalization procedure. We found that the standard C–N method was not useful in calculating excited-states because the convergence speed was practically zero when we required the numerical precision to be 10 digits. However, with the relaxed C–N method, the excited-state eigenvalues were successfully found, with the speed being 10 times slower than the time needed to find the ground-state. The amount of time required to calculate excited-states was no longer than 10 min with a Pentium IV CPU.

3. The inverse-iteration method

In this section, we use the inverse-iteration method [18] in order to calculate the excited-state eigenvalues and eigenfunctions systematically and more efficiently. Let us consider the following inverted operator:

$$\frac{1}{\mathcal{H}-\beta}, \tag{4}$$

where β is an arbitrary real number in the eigenvalue space. We apply the operator in Eq. (4) to the wave packet k times,

$$\left(\frac{1}{\mathcal{H}-\beta}\right)^k u(\rho) = \sum_{i=1}^{\infty} \frac{C_i}{(\zeta_i-\beta)^k} u_i(\rho), \tag{5}$$

where we assume that the time independent wave packet $u(\rho)$ can be expressed as a linear combination of the eigenfunctions $u_i(\rho)$ with coefficients C_i. This is closely related to the well-known power iteration scheme [18]. The β has to be chosen in such a way that the inverse operator $(\mathcal{H}-\beta)^{-1}$ can amplify the desired eigenstate selectively. Namely, for $\beta = \zeta_i + \epsilon$ such that $|\epsilon| \ll 1$, we have

$$\left|\frac{1}{\zeta_i-\beta}\right| \gg \left|\frac{1}{\zeta_j-\beta}\right|, \tag{6}$$

when $j \neq i$. Therefore, Eq. (4) plays a role as an amplifier that magnifies contributions from the term with the nearest eigenvalue from the point β. In this way, all the eigenvalues within an arbitrary range in β can be found systematically, by running β within the range. We call this approach as an *inverse-iteration C–N method* in this paper. Advantages of this method are as follows. First, the calculations of excited-states can be carried out systematically by stepping through different values of β. Second, the computing time for calculating excited-state wave functions is similar to the time needed for the calculation of the ground-state wave function. Furthermore, it does not lose accuracy in the calculation of higher-state eigenvalues while other methods do often. This contrasts the inverse-iteration C–N method to the relaxed C–N method. With the relaxed C–N method, the Gram–Schumidt orthonormalization slowed down the computing speed by 10 times, as mentioned before, and it limited the applicability of the method for excited-states. On the other hand, one may argue that with the inverse-iteration C–N method, the convergence for a given excited-state may not be guaranteed without any prior knowledge of the spectrum. That is, if the spectral properties are not known, this approach may not be useful. We found that in practice, all eigenstates within the range of interest for known problems such as the Coulomb and the linear potential problems were easily found by running β. The second weakness of this method is that it cannot be used for finding orthonormalized wave functions that belong to a degenerate set.

First, we tested the inverse-iteration C–N method on the pure Coulomb potential and to the pure linear potential ($\lambda = 0$) where the exact eigenvalues were known for both cases. This is a good benchmark because we can directly examine the performance of the algorithm by comparing the exact solutions to the numerical results of the algorithm to be tested. We found that the numerical values of eigenvalues agreed well with known analytic values, up to eleven digits. Second, we applied the inverse-iteration C–N method to the

Table 2
Numerical values of eigenvalues and the error estimation for various excited-states with the Cornell potential

State	ζ (this work)	$\Delta\zeta$
1S	1.397875641659581	3.8×10^{-13}
2S	3.475086545392783	3.4×10^{-12}
3S	5.032914359529781	6.3×10^{-12}
4S	6.370149125476954	9.4×10^{-12}
5S	7.574932640578566	1.3×10^{-11}
1P	2.825646640702388	1.2×10^{-12}
2P	4.461863593453813	3.1×10^{-12}
3P	5.847634227299904	5.5×10^{-12}
1D	3.850580006802002	5.9×10^{-13}
2D	5.292984139 140243	2.0×10^{-12}

The inverse-iteration C–N method is used to calculate eigenvalues. The Coulombic parameter is set to $\lambda = 1.0$ and the number of grid points to be $N = 300{,}000$. An estimate on the numerical errors of the computation $\Delta\zeta$ is also listed at the last column and will be discussed later.

Cornell potential and reproduced the result in Table 1. We found that eleven digits of the eigenvalues were reproduced completely from $\lambda = 0.0$ to 1.8. This is consistent with our error estimation that is to be explained later. Third, we applied the inverse-iteration C–N method to the calculation of the excited-states. Table 2 shows the eigenvalues we obtained. Note that for the 1S state in Table 2, we can compare the eigenvalue with the corresponding number in Table 1. Only the last two digits are different, which is again consistent with our error estimation. For the ground-state, the relaxed and the inverse-iteration C–N methods required similar amount of computing time, but for the excited-states, the inverse-iteration C–N method was faster by 10 times. We checked the computing speed for the Coulomb, linear, and Cornell potentials separately and all three gave similar performance.

4. Error estimation

There are two major sources of errors in our numerical calculation. One is the cut-off (ρ_{max}) and the other is the discretization of continuous equations. The cut-off gives an imperfect numerical integration but could in principle be reduced as small as possible by increasing the value of ρ_{max}. We estimated the error due to the finite value of ρ_{max} for the Coulomb and linear potentials, respectively, by integrating the exact eigenfunctions. We found that the errors were 10^{-15} or smaller when $\rho_{\text{max}} = 20$, for example. In fact, for the practical purpose, we controlled the value of ρ_{max} in such a way that the numerical error due to the finite value of ρ_{max} was smaller than the error from the discretization of continuous equations. Certainly, this assumes that the error estimates with the Coulomb and linear potentials individually are not significantly different from the errors due to the Cornell potential. Practically, selecting proper values of ρ_{max} is important, because values that are too small cause large errors and too large values may slow down the computation. We found that $\rho_{\text{max}} = 30$ was an optimal value for most of our applications discussed in this paper. Note that $\rho_{\text{max}} = 30$ corresponds to 30 times of the Bohr radius in the hydrogen atom problem, for example.

A more serious source of the error is originated from the discretization of continuous differential equations. In this paper, the differentiation and integration of wave functions are discretized with the following prescriptions [14]

$$u''_j = \frac{u_{j+1} - 2u_j + u_{j-1}}{\Delta\rho^2} + \mathcal{O}(\Delta\rho^2), \tag{7}$$

$$\int \mathrm{d}\rho u(\rho) = \frac{\Delta\rho}{2}\sum_{j=1}^{N}(u_{j+1} + u_j) + \mathcal{O}(\Delta\rho^2), \tag{8}$$

where $\Delta\rho$ is the distance between two nearest discrete points in the calculation. From both Eqs. (7) and (8), numerical errors contained in the discretization are proportional to $\Delta\rho^2 = N^{-2}$ where N is the number of grid points in the discretization. Therefore, the error in the calculation of eigenvalues due to the discretization may be approximated as

$$\Delta\zeta(N) \approx cN^{-2}, \tag{9}$$

where $\Delta\zeta(N) = |\zeta_{\text{exact}} - \zeta(N)|$ and the constant c depends on the potential. If we select two arbitrary values in grid points, N_1 and N_2, for example, then we can easily obtain the constant c as

$$c \approx \left|\frac{\Delta\zeta(N_1) - \Delta\zeta(N_2)}{N_1^{-2} - N_2^{-2}}\right| = \left|\frac{\zeta(N_1) - \zeta(N_2)}{N_1^{-2} - N_2^{-2}}\right|. \tag{10}$$

With the help of Eq. (10), we can estimate the error due to the discretization described in Eqs. (7) and (8). We refer to it as an error estimation from the power counting rule. In Fig. 1, our estimate of the numerical error $\Delta\zeta(N)$ is compared with the true error, $|\zeta_{\text{exact}} - \zeta(N)|$ for the Coulomb and the linear potentials. Here we used results of our inverse-iteration C–N method for the error analysis. It is apparent from Fig. 1 that our error estimate is accurate down to 10^{-11} for the 1S state under the Coulomb potential, for example, when $N = 300{,}000$. For others, the results are better than that of the 1S state as shown in Fig. 1. For the 1D state under the Coulomb potential, the true error looks unstable at a large value of N. This is due to the limitation in storing significant digits during our computation of $\zeta(N)$, which means it reaches a limit because of the

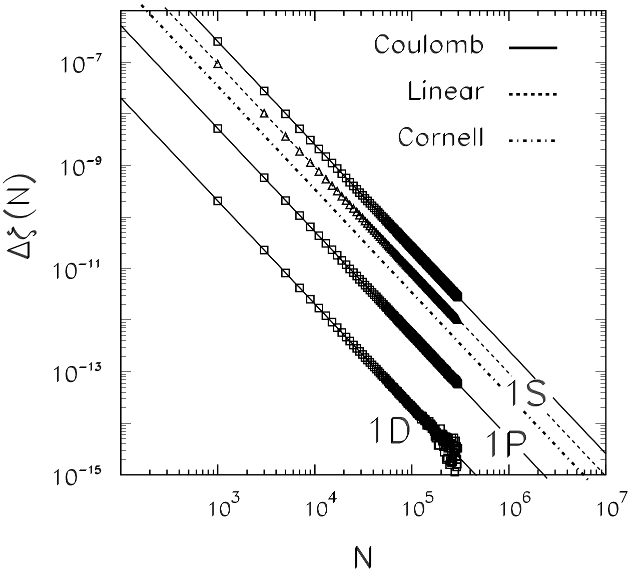

Fig. 1. The numerical error estimation for the eigenvalues as a function of the number of grid points. For the Coulomb (linear) potential, $|\zeta_{\text{exact}} - \zeta(N)|$ is indicated with open boxes (triangles) for 1S, 1P and 1D states (the 1S state only for the linear potential). The error estimates based on Eq. (9) for the Coulomb, linear and Cornell potentials are shown in straight, dashed and dot-dashed lines, respectively. Note that both axes are in logarithmic scales.

floating point precision of double size real variables that we used in the computation. Note that for the Cornell potential, the true errors cannot be calculated because the exact solutions are unknown. For the Cornell potential, we estimated that the errors were in the range of 10^{-12} as in Fig. 1. We used this error estimation technique throughout the work described in this paper. Numerical values of the error estimates are included in Tables 1 and 2.

In addition to the spatial contribution to the error described above, the finite time evolution may also contribute. However, in our study, the time evolution is always kept until the fluctuation of the eigenvalue is much smaller than our target precision defined by Eq. (9). Therefore, little contribution due to the finite evolution exists in our error estimation.

5. Conclusions

We have presented two numerical approaches for calculating the Schrödinger equation with the Crank–Nicolson method. In the relaxed C–N method, the time evolution operator was re-interpreted as a weighting operator for finding the ground-state eigenfunction more precisely. Second, the inverse-iteration method was applied to the C–N method that was more efficient in computing not only the ground-state but also the excited-state wave functions systematically. At the end, an absolute error estimation method was developed based on a power counting rule that was consistent with absolute error values when exact solutions are known. These two algorithms may be useful when precise numerical results are required. Possible applications may include Cornell potential [8,9] and Bose-Einstein condensation of trapped atomic vapors [4].

Acknowledgments

We thank Jungil Lee for his suggestion on this topic and Q-Han Park and Ki-Hwan Kim for useful discussion on the numerical treatment. E.W. is indebted to Tai Hyun Yoon for his critical comments on this manuscript. D.K.'s research was supported by the Korea Research Foundation Grant funded by the Korean Government (MOEHRD), (KRF-2006-612-C00003). E.W.'s research was supported by Grant No. R01-2005-000-10089-0 from the Basic Research Program of the Korea Science & Engineering Foundation.

References

[1] C.H. Mehta, S.H. Patil, Phys. Rev. A 17 (1978) 34.
[2] E.R. Vrscay, Phys. Rev. A 31 (1985) 2054.
[3] S.C. Chhajlany, D.A. Letov, Phys. Rev. A 44 (1991) 4725.
[4] M.L. Chiofalo, S. Succi, M.P. Tosi, Phys. Rev. E 62 (2000) 7438.
[5] L. Lehtovaara, T. Kiljunen, J. Eloranta, J. Comput. Phys. 194 (2004) 78.
[6] Q. Chang, E. Jia, W. Sun, J. Comput. Phys. 148 (1999) 397.
[7] N. Watanabe, M. Tsukada, Phys. Rev. E 62 (2000) 2914.
[8] E. Eichten, K. Gottfried, T. Kinoshita, K.D. Lane, T.M. Yan, Phys. Rev. D 17 (1978) 3090;
E. Eichten, K. Gottfried, T. Kinoshita, K.D. Lane, T.M. Yan, Phys. Rev. D 21 (1980) 313(E).
[9] E. Eichten, K. Gottfried, T. Kinoshita, K.D. Lane, T.M. Yan, Phys. Rev. D 21 (1980) 203.
[10] J.W. Norbury, K.M. Maung, D.E. Kahana, Phys. Rev. A 50 (1994) 2075.
[11] A. Tang, J.W. Norbury, Phys. Rev. E 63 (2001) 066703.
[12] S. Jacobs, M.G. Olsson, C. Suchyta III, Phys. Rev. D 33 (1986) 3338;
S. Jacobs, M.G. Olsson, C. Suchyta III, Phys. Rev. D 34 (1986) 3536(E).
[13] R. Roychoudhury, Y.P. Varshni, M. Sengupta, Phys. Rev. A 42 (1990) 184.
[14] W.H. Press, B.P. Flannery, S.A. Teukolsky, W.T. Vetterling, Numerical Recipes in C: The Art of Scientific Computing, Cambridge University Press, 1992.
[15] I. Galbraith, Y.S. Ching, E. Abraham, Am. J. Phys. 52 (1984) 60.
[16] Peter Hansbo, J. Comput. Phys. 159 (2000) 274.
[17] G.T. Bodwin, D. Kang, J. Lee, Phys. Rev. D 74 (2006) 014014.
[18] M.T. Heath, Scientific Computing: An Introductory Survey, McGraw Hill, 2002.